Nanoscale

PAPER

View Article Online
View Journal | View Issue

Cite this: *Nanoscale*, 2014, **6**, 8306

Field electron emission of layered Bi_2Se_3 nanosheets with atom-thick sharp edges†

Huihui Huang,‡[ab] Yuan Li,‡[c] Qi Li,‡[c] Borui Li,[a] Zengcai Song,[a] Wenxiao Huang,[c] Chujun Zhao,[b] Han Zhang,*[b] Shuangchun Wen,[b] David Carroll*[c] and Guojia Fang*[a]

Received 12th November 2013
Accepted 5th May 2014

DOI: 10.1039/c3nr06015b

www.rsc.org/nanoscale

Field electron emission properties of solution processed few-layer Bi_2Se_3 nanosheets are studied for the first time, which exhibit a low turn-on field of 2.3 V μm^{-1}, a high field enhancement factor of up to 6860 and good field emission stability. This performance is better than that of the as reported layered MoS_{2f} sheets and is comparable to that of single layer graphene films. The efficient field emission behaviours are found to be not only attributed to their lower work function but also related to their numerous sharp edges or protrusion decorated structure based on our simulation results. Besides, the contribution of possible two-dimensional electron gas surface states of atom-thick layered Bi_2Se_3 nanosheets is discussed in this paper. We anticipate that these solution processed layered Bi_2Se_3 nanosheets have great potential as robust high-performance vertical structure electron emitters for future light weight and highly flexible vacuum micro/nano-electronic device applications.

1. Introduction

Field electron emission is a phenomenon that involves extracting electrons from materials *via* quantum tunnelling through the surface potential barrier under a strong electric field. Its applications include flat-panel displays, high energy accelerators, X-ray sources, microwave amplifiers and vacuum microelectronic devices.[1–3] Among the field emission materials, one-dimensional (1D) nanostructure materials including ZnO, carbon nanotubes or nanowires have been sufficiently studied for many years.[4–10] Field emission from two-dimensional (2D) atomic crystal materials such as graphene[11–16] and MoS_2[17] has recently attracted immense interest due to their atom-thick sharp edges, unique electronic properties and compatibility with planar device technology.

Most recently, V_2VI_3 compounds like Bi_2Se_3, Bi_2Te_3 and Sb_2Te_3 have received growing attention not only because of their thermoelectric properties but also their unique electronic properties with insulating bulk states and topologically protected single Dirac cone surface states, namely, topological insulators (TIs).[18–23] Besides, these materials have layered structures due to the weak van der Waals' force between the quintuple layers (QLs) along the [001] direction. As the thickness reduces to a few QLs, its surface properties could be enhanced due to the increase of the ratio of surface area to volume.[18–23] For Bi_2Se_3, for example, recent literature reported that the square resistance of Bi_2Se_3 nanosheets with a few QLs could be as low as 330 Ω, which might be ascribed to a new type of two-dimensional electron gas (2DEG) covered on the surface.[21] The good conductivity and large surface to volume ratio (more atom-thick sharp edges or boundaries) of a layered Bi_2Se_3 nanosheet indicate that it could be a promising excellent field emission material. Field emission properties of Bi_2Se_3 nanoflake arrays prepared by vapour phase growth have been reported.[24] However, field emission properties of Bi_2Se_3 with atom-thick 2D layered structures have not been reported from experiment or theory. In this paper, we experimentally studied the field emission properties of solution processed layered Bi_2Se_3 nanosheets and proposed a theoretical field emission model for this system.

2. Results and discussion

Layered Bi_2Se_3 nanosheets were prepared from bulk Bi_2Se_3 crystals by a three-step exfoliation method including mechanical grinding, hydrothermal exfoliation and sonication exfoliation (see the fabrication route in Fig. S1†). Fig. 1(a)–(c) show the transmission electron microscopy (TEM) images of the layered Bi_2Se_3 nanosheets, which were prepared by directly dropping onto the substrate from the dispersion solution (see Fig. S1(d)†). Clearly layered structures with sizes of several hundred nanometres could be seen from these images. Furthermore, the

[a]*Key Lab of Artificial Micro- and Nano-Structures of Ministry of Education of China, Department of Electronic Science & Technology, School of Physics and Technology, Wuhan University, Wuhan 430072, P. R. China. E-mail: gjfang@whu.edu.cn*

[b]*College of Optoelectronic Engineering, Shenzhen University, Shenzhen 518060, P. R. China. E-mail: hzhang@szu.edu.cn*

[c]*Center for Nanotechnology and Molecular Materials, Department of Physics, Wake Forest University, Winston-Salem, NC 27109, USA. E-mail: carroldl@wfu.edu*

† Electronic supplementary information (ESI) available. See DOI: 10.1039/c3nr06015b

‡ These authors contributed equally to this work.

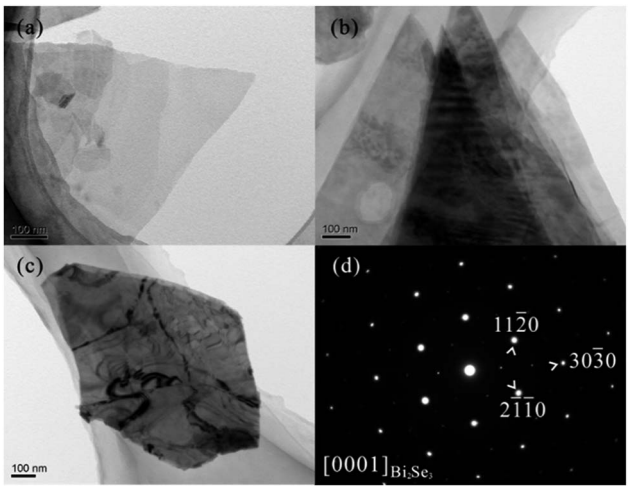

Fig. 1 (a–c) TEM images of the layered Bi_2Se_3 nanosheets. (d) SAED pattern of the layered Bi_2Se_3 nanosheets.

corresponding selected area electron diffraction (SAED) pattern of the Bi_2Se_3 nanosheets is shown in Fig. 1(d). The regular shape of the SAED pattern reveals that the layered Bi_2Se_3 nanosheets are monocrystalline and the wide surfaces are analyzed as {001} planes, which implies that the nanosheets were exfoliated along the [001] (*c*-axis) direction.

Fig. 2 shows the scanning electron microscopy (SEM) images of layered Bi_2Se_3 nanosheets which were spin-coated on a Si substrate from the dispersion solution (see Fig. S1(d)†). Flat layered Bi_2Se_3 nanosheets were dispersed on the Si substrate with sizes up to several hundred nanometers. In order to prove the atom-thick layered structure of the as-obtained Bi_2Se_3 nanosheets, atomic force microscopy (AFM) techniques were applied to the sample, which is shown in Fig. 3. Fig. 3(a) shows the AFM image of dispersed layered Bi_2Se_3 nanosheets; the thicknesses of all the nanosheets in the image are smaller than 2.87 nm. For accurate thickness information, height profiles of line A–B and line C–D in the image are shown in Fig. 3b and c. The thicknesses of the samples in line A–B and line C–D are calculated as ~1.0 nm and ~1.3 nm, respectively. Considering the instrumental error, these results imply that the Bi_2Se_3 nanosheets in the image might be made up of 1 or 2 QLs since each planar QL has a thickness of ~0.955 nm.[25] These above results prove that the as-prepared Bi_2Se_3 nanosheets have atom-thick 2D layered structures.

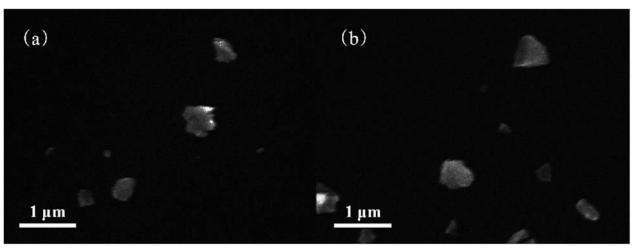

Fig. 2 SEM images of the exfoliated layered Bi_2Se_3 nanosheets spin-coated on a Si substrate.

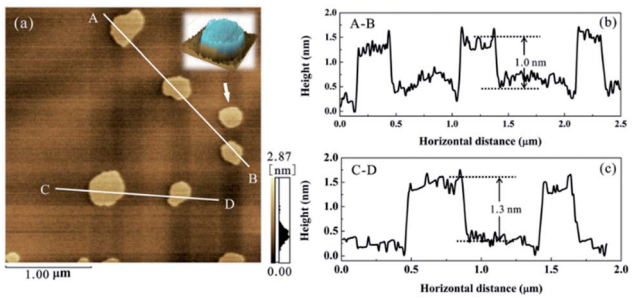

Fig. 3 (a) AFM image and height profile (b–c) of the layered Bi_2Se_3 nanosheets.

Furthermore, Fig. 4(a) compares the Raman spectra of the layered and bulk Bi_2Se_3 in the range of 50–200 cm^{-1}. The three Raman peaks centred at ~70 cm^{-1}, ~130 cm^{-1} and ~173 cm^{-1} could be assigned to the out-plane vibrational mode (A_{1g}^1), the in-plane vibrational mode (E_g^2), and the out-plane vibrational mode (A_{1g}^2) of Bi_2Se_3, respectively.[26,27] It also can be seen that the relative intensity of the A_{1g}^1 vibrational mode in the layered Bi_2Se_3 spectrum is stronger than that in the bulk Bi_2Se_3 spectrum. Besides, the line width (~11.8 cm^{-1}) of the E_g^2 vibrational mode of the layered Bi_2Se_3 is a little bit broader than that of the bulk Bi_2Se_3 (~10.5 cm^{-1}). These Raman results confirm the few layer structure of the Bi_2Se_3.[27]

In order to investigate the surface electronic states of Bi_2Se_3, ultraviolet photoelectron spectroscopy (UPS) spectra of layered Bi_2Se_3 and bulk Bi_2Se_3 are compared in Fig. 4(b). On one hand, the UPS spectrum of layered Bi_2Se_3 shifted by about 0.4 eV to

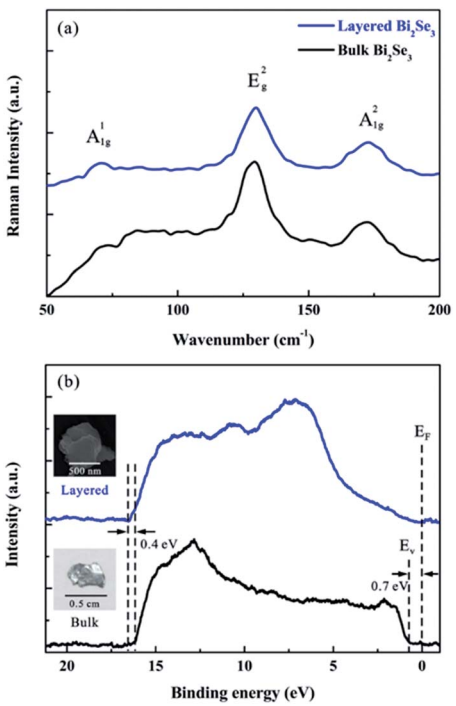

Fig. 4 (a) Raman spectra of layered Bi_2Se_3 and bulk Bi_2Se_3. (b) UPS spectra of layered Bi_2Se_3 and bulk Bi_2Se_3.

higher binding energy compared with that of bulk Bi_2Se_3, indicating a decrease in work function for the layered Bi_2Se_3. On the other hand, the valence band maximum (E_v) of bulk Bi_2Se_3 is located 0.7 eV below its Fermi level (E_F), indicating that the bulk conduction band is occupied due to the n-type doping of defects, which also implies that the surface properties of bulk Bi_2Se_3 (with a band gap of ~0.3 eV) might be masked by its bulk states. However, no clear energy gap between E_v and E_F could be found in the UPS spectrum of layered Bi_2Se_3, which might be caused by the dominating zero-band surface states of the layered Bi_2Se_3 due to its large surface-to-volume ratio. The lower work function and the possible much more conductive surface of layered Bi_2Se_3 should be related to the changed surface properties including surface energy and surface band structure,[21,22] both of which are conducive to the field emission and it will be proved in the following experiments.

The electron-field-emission measurement of the layered Bi_2Se_3 nanosheets was carried out in a vacuum chamber with a base pressure lower than 1×10^{-5} Pa at room temperature. In this case, the Bi_2Se_3 nanosheets were spin-coated on pre-cleaned n-type silicon (9.0×10^{-3} Ω cm) from the dispersion solution (see Fig. S1(d)†). Therefore, the Bi_2Se_3/Si was employed as the cathode and an ITO glass was used as the anode for this measurement. A typical plot of field emission current density *versus* electric field (*J*–*E*) curve at a vacuum gap of ~220 μm is shown in Fig. 5(a). As compared in Table 1, the turn-on field (E_{to}) of the layered Bi_2Se_3 on flat Si (defined as the emission current density reaching 10 μA cm^{-2}) is about 2.3 V μm^{-1}, which is smaller than those of layered MoS_2 sheets and is comparable to that of single-layer graphene films.[11,17] The obtained *J*–*E* curve could be further analyzed by the Fowler–Nordheim (FN) theory, which can be expressed by the following equation:

$$J = A(\beta^2 E_0^2/\phi)\exp(-B\phi^{3/2}/\beta E_0) \quad (1)$$

where *J* is the field emission current density, E_0 is the mean field between the cathode and anode, β is the field enhancement factor, ϕ is the work function, and *A* and *B* are constants ($A = 1.54 \times 10^{-6}$ A eV V^{-2}, $B = 6.83 \times 10^3$ V $eV^{-3/2}$ μm^{-1}). The inset of Fig. 5(a) shows the corresponding FN plot ($\ln(1/E_0^2)$ *vs.* $1/E_0$), which shows approximately a linear relationship with a slope $m = -10.1$. Since the work function of layered Bi_2Se_3 could be deduced from the UPS results as 4.7 eV, the field enhancement factor β can be calculated to be 6860 ($\beta = (-6.8 \times 10^3)\phi^{3/2}/m$), which is larger than those of single-layer graphene films and layered MoS_2 sheets, as shown in Table 1. The emission stability test was performed at a preset value of ~0.13 mA cm^{-2} and the recording interval was 1 s. As shown in Fig. 5(b), no obvious emission degradation is observed for over 3600 s and the emission fluctuation is about ~15%. The inset of Fig. 5(b) illustrates the corresponding electron emission fluorescence image. In the meantime, we also fabricated a flexible field emitter simply by drop casting the layered Bi_2Se_3 dispersion onto carbon cloth (see Fig. S4–S7†), which has a low turn-on field of 2.3 V μm^{-1}, a field enhancement factor of 3207, a large field emission current close to 6 mA cm^{-2} and good emission stability (see Fig. S6†).

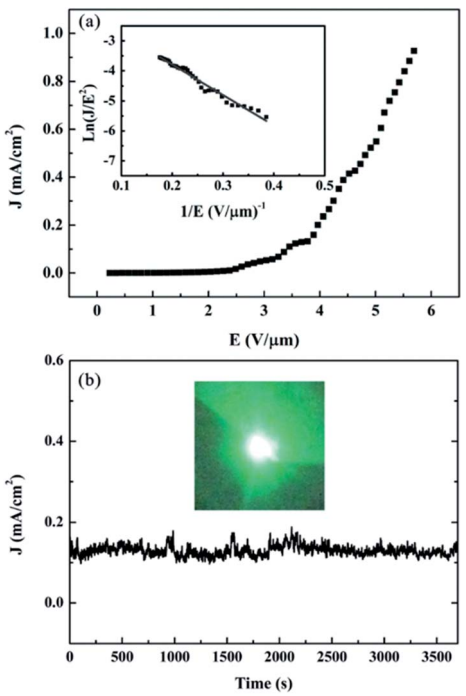

Fig. 5 (a) Typical plot of field emission current density *versus* electric field (*J*–*E*) of the layered Bi_2Se_3 nanosheets. The inset is the corresponding Fowler–Nordheim (FN) plot. (b) The field emission current stability of the layered Bi_2Se_3 nanosheets over time; the inset is an electron emission fluorescence image of the layered Bi_2Se_3 nanosheet emitter (a phosphor coated ITO glass was used as the anode in this case).

In order to investigate the origin of the efficient field emission behaviours of layered Bi_2Se_3 nanosheets, we further proposed a field emission model based on a finite element method with ANSYS v14 software and Comsol 4.3 software.[28] There are two very important issues in the model of layered Bi_2Se_3 field emission: (1) the electrical field distribution on the layered Bi_2Se_3 in field emission and (2) the shape dependence of layered Bi_2Se_3.

First, we simulated the electrical field intensity distributed on a regular circular layered Bi_2Se_3 with a positive voltage of 1000 V applied to the anode (see Fig. S8†). Based on these parameters, especially the permittivity of the involved materials (see Table S1 in the ESI†), the edge effect is clearly proved in Fig. 6(a) with a maximum intensity of 6.3 V μm^{-1}. This also shows that the edge effect is the key point to field emission of layered structural materials. Therefore, could we make more edges to strengthen the effect? We further investigated the irregular shape with more edges, and compared it with the regular shape (circular disc). Fig. 6(b) and (c) compare the electrical field distributions of two cases. Obviously, the irregular shape shows a much more obvious intense edge effect. This probably provides a way to enhance the field emission for layered materials, because unlike bulk materials used in field emission having a tip in the *z* direction, layered materials show a plane on the top, meaning that it is very difficult to improve

Table 1 Comparison between the performances of relevant field emitters and the layered Bi_2Se_3 nanosheets in this work

	Turn-on field (V μm^{-1})	Field enhancement factor (β)	Reference
Single-layer graphene films	2.3 (@10 μA cm^{-2})	3700	11
Layered MoS_2 sheets	3.5 (@10 μA cm^{-2})	1138	17
Layered Bi_2Se_3 on flat Si	2.3 (@10 μA cm^{-2})	6860	This work
Layered Bi_2Se_3 on flexible carbon cloth	2.3 (@10 μA cm^{-2})	3207	This work

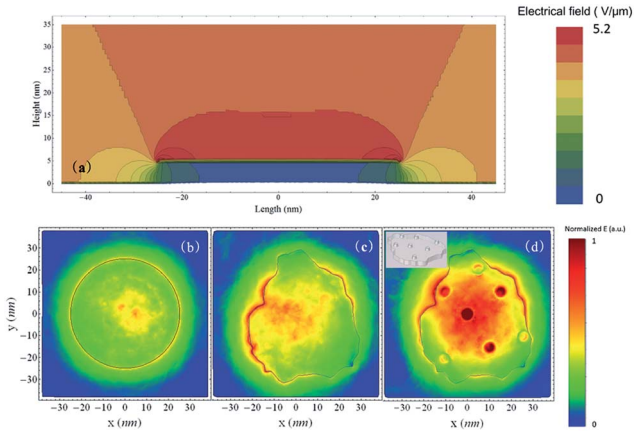

Fig. 6 (a) Sectional drawing of electrical field distribution on a Bi_2Se_3 layer (5 nm thickness, 50 nm diameter); (b–d) electrical field distributions for layered Bi_2Se_3 with regular shape (b), irregular shape (c) and protrusion decorated structure (d).

field emission through making a tip toward the z direction. In terms of the inspiration from Fig. 6(b) and (c), the field emission in a layered material can be tuned *via* making edges in the crosswise dimension (x and y direction), which is in accordance with the experimental results since the solution processed layered Bi_2Se_3 nanosheets have complicated irregular shapes (see Fig. 1–3). Besides, we also simulated the protrusion decorated structure in Fig. 6(d), which shows further field enhancements over the sharp edge structures (see Fig. 6(c)). The above simulation results reveal that the efficient field emission properties of layered Bi_2Se_3 nanosheets fabricated in this work are not only related to their possible 2DEG in the surface and lower work function but also to their abundant sharp edges or protrusion decorated structure.

3. Experimental

Layered Bi_2Se_3 nanosheet synthesis

Layered Bi_2Se_3 nanosheets were prepared from bulk Bi_2Se_3 crystals by a three-step exfoliation method. First, bulk Bi_2Se_3 crystals (Alfa Aesar) were ground into Bi_2Se_3 powders using an agate mortar (from Fig. S1(a) and (b)†). Then, the Bi_2Se_3 powders were converted into Bi_2Se_3 nanosheet clusters (from Fig. S1(b) and (c)†) by a hydrothermal intercalation and exfoliation method[29] as follows: Bi_2Se_3 powders were placed into a sealed Teflon-lined autoclave with an ethylene glycol solution of lithium hydroxide (8 M). After the autoclave was oven-heated at 200 °C for 24 h, Bi_2Se_3 nanosheet clusters were obtained by centrifugation and rinsed with acetone and deionized water to eliminate the residual lithium hydroxide. At last, to get a uniform dispersion of layered Bi_2Se_3 nanosheets, the as-prepared Bi_2Se_3 nanosheet clusters were dried and immediately suspended in isopropanol and sonicated for 30 min to achieve final exfoliation (from Fig. S1(c) and (d)†).

Layered Bi_2Se_3 nanosheet characterization

The morphologies were characterized by Sirion field emission scanning electron microscopy (SEM: Philips XL30). Transmission electron microscopy (TEM) techniques, including the selected area electron diffraction (SAED), were performed using a JEM-2010 electron microscope. Atomic Force Microscopy (AFM) measurements were carried out in a SPM-9500J3 system. Raman spectra were obtained using a Horiba-Jobin-Yvon Lab-Raman HR confocal microscope using 488 nm laser excitation at room temperature. X-ray photoelectron spectroscopy (XPS) and ultraviolet photoelectron spectroscopy (UPS) studies were conducted with a Thermo ESCALAB 250xi instrument.

Field emission measurement

Field emission measurements were performed with a two-parallel-plate configuration (Bi_2Se_3/Si as the cathode and a phosphor coated ITO glass as the anode) in a vacuum chamber with base pressure lower than 2.0×10^{-5} Pa. The cathode and the anode were separated by a 220 μm thick Teflon spacer, and the cathode area was 0.04 cm^2. The current–voltage (I–V) characteristics were measured using a Keithley 6485 picoammeter and a Keithley 248 high voltage supply.

4. Conclusions

In summary, layered Bi_2Se_3 nanosheets were prepared from Bi_2Se_3 crystals by a three-step exfoliation method. Field emission with a low turn-on field of 2.3 V μm^{-1}, a high field enhancement factor of 6860 and good field emission stability was observed from the layered Bi_2Se_3 nanosheets. We further proposed a field emission model to investigate the origin of its efficient field emission behaviours, which found that the sharp and irregular shapes of exfoliated atom-thick layered Bi_2Se_3 nanosheets play a key role in the edge effect that results in its efficient field emission. This work suggests that layered Bi_2Se_3 nanosheets with atom-thick sharp edges have great potential as high-performance vertical structure field emitters for a future

light weight and highly flexible electron source such as vacuum electronic device applications.

Acknowledgements

This work was supported by the 973 Program (2011CB933300) of China, the National Natural Science Foundation of China (61376013, 11074194, J1210061). The authors would like to thank Dr Wei Zeng for his help in coding the program of ANSYS.

Notes and references

1 W. B. Choi, D. S. Chung, J. H. Kang, H. Y. Kim, Y. W. Jin, I. T. Han, Y. H. Lee, J. E. Jung, N. S. Lee, G. S. Park and J. M. Kim, *Appl. Phys. Lett.*, 1999, **75**, 3129.
2 K. L. Jensen, *Phys. Plasmas*, 1999, **6**, 2241.
3 C. Hernandez-Garcia, M. L. Stutzman and P. G. O'Shea, *Phys. Today*, 2008, **61**, 44.
4 N. S. Xu and S. E. Huq, *Mater. Sci. Eng. R*, 2005, **48**, 47.
5 W. A. de Heer, A. Châtelain and D. Ugarte, *Science*, 1995, **270**, 1179.
6 Y. K. Tseng, C. J. Huang, H. M. Cheng, I. N. Lin, K. S. Liu and I. C. Chen, *Adv. Funct. Mater.*, 2003, **13**, 811.
7 C. J. Lee, T. J. Lee, S. C. Lyu, Y. Zhang, H. Ruh and H. J. Lee, *Appl. Phys. Lett.*, 2002, **81**, 3648.
8 X. Fang, Y. Bando, U. K. Gautam, C. Ye and D. Golberg, *J. Mater. Chem.*, 2008, **18**, 509.
9 C. Li, G. Fang, N. Liu, J. Li, L. Liao, F. Su, G. Li, X. Wu and X. Zhao, *J. Phys. Chem. C*, 2007, **111**, 12566.
10 S. Fan, M. G. Chapline, N. R. Franklin, T. W. Tombler, A. M. Cassell and H. Dai, *Science*, 1999, **283**, 512.
11 Z. S. Wu, S. Pei, W. Ren, D. Tang, L. Gao, B. Liu, F. Li, C. Liu and H. M. Cheng, *Adv. Mater.*, 2009, **21**, 1756.
12 Z. Yang, Q. Zhao, Y. Ou, W. Wang, H. Li and D. Yu, *Appl. Phys. Lett.*, 2012, **101**, 173107.
13 A. Malesevic, R. Kemps, A. Vanhulsel, M. P. Chowdhury, A. Volodin and C. Van Haesendonck, *J. Appl. Phys.*, 2008, **104**, 084301.
14 M. Qian, T. Feng, H. Ding, L. Lin, H. Li, Y. Chen and Z. Sun, *Nanotechnology*, 2009, **20**, 425702.
15 C. K. Huang, Y. Ou, Y. Bie, Q. Zhao and D. Yu, *Appl. Phys. Lett.*, 2011, **98**, 263104.
16 V. P. Verma, S. Das, I. Lahiri and W. Choi, *Appl. Phys. Lett.*, 2010, **96**, 203108.
17 R. V. Kashid, D. J. Late, S. S. Chou, Y. K. Huang, M. De, D. S. Joag, M. A. More and V. P. Dravid, *Small*, 2013, **16**, 2730.
18 H. Zhang, C. X. Liu, X. L. Qi, X. Dai, Z. Fang and S. C. Zhang, *Nat. Phys.*, 2009, **5**, 438.
19 Y. Xia, D. Qian, D. Hsieh, L. Wray, A. Pal, H. Lin, A. Bansil, D. Grauer, Y. S. Hor, R. J. Cava and M. Z. Hasan, *Nat. Phys.*, 2009, **5**, 398.
20 Y. Zhang, K. He, C. Z. Chang, C. L. Song, L. L. Wang, X. Chen, J. F. Jia, Z. Fang, X. Dai, W. Y. Shan, S. Q. Shen, Q. Niu, X. L. Qi, S. C. Zhang, X. C. Ma and Q. K. Xue, *Nat. Phys.*, 2010, **6**, 584.
21 H. Peng, W. Dang, J. Cao, Y. Chen, D. Wu, W. Zheng, H. Li, Z. X. Shen and Z. Liu, *Nat Chem.*, 2012, **4**, 281.
22 H. Peng, K. Lai, D. Kong, S. Meister, Y. Chen, X. L. Qi, S. C. Zhang, Z.-X. Shen and Y. Cui, *Nat. Mater.*, 2010, **9**, 225.
23 J. S. Son, M. K. Choi, M. K. Han, K. Park, J. Y. Kim, S. J. Lim, M. Oh, Y. Kuk, C. Park, S. J. Kim and T. Hyeon, *Nano Lett.*, 2012, **12**, 640.
24 Y. Yan, Z. M. Liao, F. Yu, H. C. Wu, G. Y. Jing, Z. C. Yang, Q. Zhao and D. P. Yu, *Nanotechnology*, 2012, **23**, 305704.
25 W. Dang, H. Peng, H. Li, P. Wang and Z. Liu, *Nano Lett.*, 2010, **10**, 2870.
26 W. Richter and C. R. Becker, *Phys. Status Solidi B*, 1977, **84**, 619.
27 J. Zhang, Z. Peng, A. Soni, Y. Zhao, Y. Xiong, B. Peng, J. Wang, M. S. Dresselhaus and Q. Xiong, *Nano Lett.*, 2011, **11**, 2407.
28 N. S. Liu, G. J. Fang, W. Zeng, H. Zhou, H. Long and X. Z. Zhao, *J. Mater. Chem.*, 2012, **22**, 3478.
29 L. Ren, X. Qi, Y. Liu, G. Hao, Z. Huang, X. Zou, L. Yang, J. Li and J. Zhong, *J. Mater. Chem.*, 2012, **22**, 4921.

